BMC Genomics

BioMed Central

Research article

Refined physical map of the human *PAX2/HOX11/NFKB2* cancer gene region at 10q24 and relocalization of the *HPV6AIL* viral integration site to 14q13.3-q21.1

Sheryl M Gough[1], Margaret McDonald[1], Xiao-Ning Chen[2], Julie R Korenberg[2], Antonino Neri[3], Tomas Kahn[4], Michael R Eccles[5] and Christine M Morris*[1]

Address: [1]Cancer Genetics Research Group, Christchurch School of Medicine & Health Sciences, Christchurch, New Zealand, [2]Departments of Human Genetics and Pediatrics, UCLA and Cedars-Sinai Medical Center, Los Angeles, USA, [3]Laboratory of Experimental Hematology and Molecular Genetics, Ospedale Policlinico, IRCCS, University of Milan, School of Medicine, Milan, 20122 Italy, [4]Deutsches Bank AG, Expert Team Life Sciences, P7, 10-15, D-68161 Mannheim, Germany and [5]Pathology Department, Dunedin School of Medicine, University of Otago, Dunedin, New Zealand

Email: Sheryl M Gough - sheryl.gough@chmeds.ac.nz; Margaret McDonald - margaret.mcdonald@chmeds.ac.nz; Xiao-Ning Chen - Xiao-Ning.Chen@cshs.org; Julie R Korenberg - Julie.Korenberg@cshs.org; Antonino Neri - neri.a@policlinico.mi.it; Tomas Kahn - tomas.kahn@db.com; Michael R Eccles - Michael.Eccles@stonebow.otago.ac.nz; Christine M Morris* - christine.morris@chmeds.ac.nz

* Corresponding author

Published: 3 March 2003

BMC Genomics 2003, **4**:9

Received: 26 November 2002

Accepted: 3 March 2003

This article is available from: http://www.biomedcentral.com/1471-2164/4/9

Abstract

Background: Chromosome band 10q24 is a gene-rich domain and host to a number of cancer, developmental, and neurological genes. Recurring translocations, deletions and mutations involving this chromosome band have been observed in different human cancers and other disease conditions, but the precise identification of breakpoint sites, and detailed characterization of the genetic basis and mechanisms which underlie many of these rearrangements has yet to be resolved. Towards this end it is vital to establish a definitive genetic map of this region, which to date has shown considerable volatility through time in published works of scientific journals, within different builds of the same international genomic database, and across the differently constructed databases.

Results: Using a combination of chromosome and interphase fluorescent in situ hybridization (FISH), BAC end-sequencing and genomic database analysis we present a physical map showing that the order and chromosomal orientation of selected genes within 10q24 is CEN-*CYP2C9-PAX2-HOX11-NFKB2*-TEL. Our analysis has resolved the orientation of an otherwise dynamically evolving assembly of larger contigs upstream of this region, and in so doing verifies the order and orientation of a further 9 cancer-related genes and *GOT1*. This study further shows that the previously reported human papillomavirus type 6a DNA integration site HPV6AI1 does not map to 10q24, but that it maps at the interface of chromosome bands 14q13.3-q21.1.

Conclusions: This revised map will allow more precise localization of chromosome rearrangements involving chromosome band 10q24, and will serve as a useful baseline to better understand the molecular aetiology of chromosomal instability in this region. In particular, the relocation of HPV6AI1 is important to report because this HPV6a integration site, originally isolated from a tonsillar carcinoma, was shown to be rearranged in other HPV6a-related

malignancies, including 2 of 25 genital condylomas, and 2 of 7 head and neck tumors tested. Our finding shifts the focus of this genomic interest from 10q24 to the chromosome 14 site.

Background

The genomic interval that spans chromosome bands 10q24-q25 contains a high frequency of structural chromosome aberrations associated with cancer and development. However, existing published maps around the *PAX2/HOX11/NFKB2* region of 10q24 have differed with respect to marker and gene content, their relative order and chromosomal orientation [1–4]. More recent inconsistencies in the positioning of selected genes with respect to known markers have also been evident within the context of the human genome databases (Figure 1). It is essential to have available an accurate physical map of this region so that disease-related chromosome aberrations can be precisely localized, and to better understand the interplay of regulatory elements associated with genes that map within this domain.

The 10q24 region harbors several loci of fundamental biological importance, including the *HOX11* (*TLX1*,*TCL3*), *PAX2* and *NFKB2/LYT-10* genes. *HOX11* is an orphan homeobox gene that maps outside of the four recognized homeobox gene clusters. It encodes a DNA-binding nuclear transcription factor [5], and is involved in spleen organogenesis [6,7]. About 5% of T-cell acute lymphoblastic leukaemias (T-ALL) show chromosome translocations involving break-prone regions immediately upstream of the *HOX11* gene at 10q24 and the TCR genes at 7q35 or 14q11. *HOX11* is activated by TCR α/δ regulatory elements as a result of these rearrangements, and inappropriately expresses a 2.3 kb transcript [8–13]. *PAX2* is important during embryogenesis, and is aberrantly expressed in renal, breast and prostate tumors [14–16]. Mutations in *PAX2* are also associated with defects in eye, ear, urogenital tract and CNS development [17,18]. The nuclear factor kappa-B 2 (*NFKB2*) gene is a member of the NFKB/Rel gene family, the signaling pathways of which are recognized as pivotal to the regulation of acute inflammatory and immune responses, and increasingly to tumor development [19,20]. Translocations or structural alterations of *NFKB2* (alias *LYT-10*) have been associated with ~2% of various lymphoid malignancies, and usually result in the partial or total deletion of the carboxyl-terminal region encoding the *ankyrin* domain [21,22].

Positional cloning of a balanced t(10;19)(q24;q13) translocation found in a glioblastoma cell line has identified a new gene, *LGI1*, which is rearranged and downregulated in malignant brain tumors and has recently been implicated in autosomal dominant lateral temporal epilepsy (EPT) [23–25]. Karyotype, comparative genomic hybridization and loss of heterozygosity studies also indicate that yet to be identified oncogenes or tumor suppressor genes map to 10q24. For example, loss or rearrangement of regions encompassing 10q24 is associated with cancers of the lung [26,27], prostate [28–33], bladder [34–36], skin [37,38], and lymphatic system [39–41]. The human papillomavirus type 6a (HPV6a) was also previously reported to integrate at 10q24 in a case of tonsillar carcinoma, and rearrangements involving this locus have been indicated for other papillomavirus-associated malignancies [42].

As one part of our investigations of a novel leukaemia-related chromosomal translocation (Gough et al, unpublished), we have used a combination of chromosome and interphase FISH, BAC end-sequencing, PCR and genome database analysis to map the order and chromosomal orientation of selected cancer-related genes and the HPV6a viral integration site HPV6AI1 within 10q24. Here we present new data that confirms the order CEN-*CYP2C9-PAX2-HOX11-NFKB2*-TEL. This finding resolves the physical arrangement of larger DNA sequence contigs containing these and at least 9 other genes which have so far been implicated in different cancer subtypes. Our studies further show that HPV6AI1 does not map within 10q24, but at a different chromosomal site, namely at the interface of chromosome bands 14q13.3-q21.1.

Results

Two-Color FISH Establishes Order and Orientation of Genes and Markers at 10q24

Selected large-insert clones (refer Methods) were biotin- or digoxygenin-labeled, pooled in combinations of three, then hybridized to G1-arrested interphase nuclei. For each experiment, after signal amplification using FITC- (green) or Texas Red- (red) tagged immunofluorescent reagents, the order of signals from at least 55 chromosomes, and usually 100, was recorded. After exclusion of chromosomes showing ambiguous signal patterns, the predominant order of signals was taken to represent the physical order of the probes along the chromosome (Table 1, Figure 2a,2b,2c,2d,2e,2f,2g,2h,2i,2j,2k,2l). For many combinations, the same three probes were pooled and hybridized twice. For the first of these paired experiments, two probes were labeled with biotin and a third with digoxygenin. For the second, the probe label and detection color was reversed for two of the probes. By this alternation, and through a sequence of different probe combinations, a final arrangement of genes and markers across the 10q24 region was derived (Table 1, Figures 1d,2).

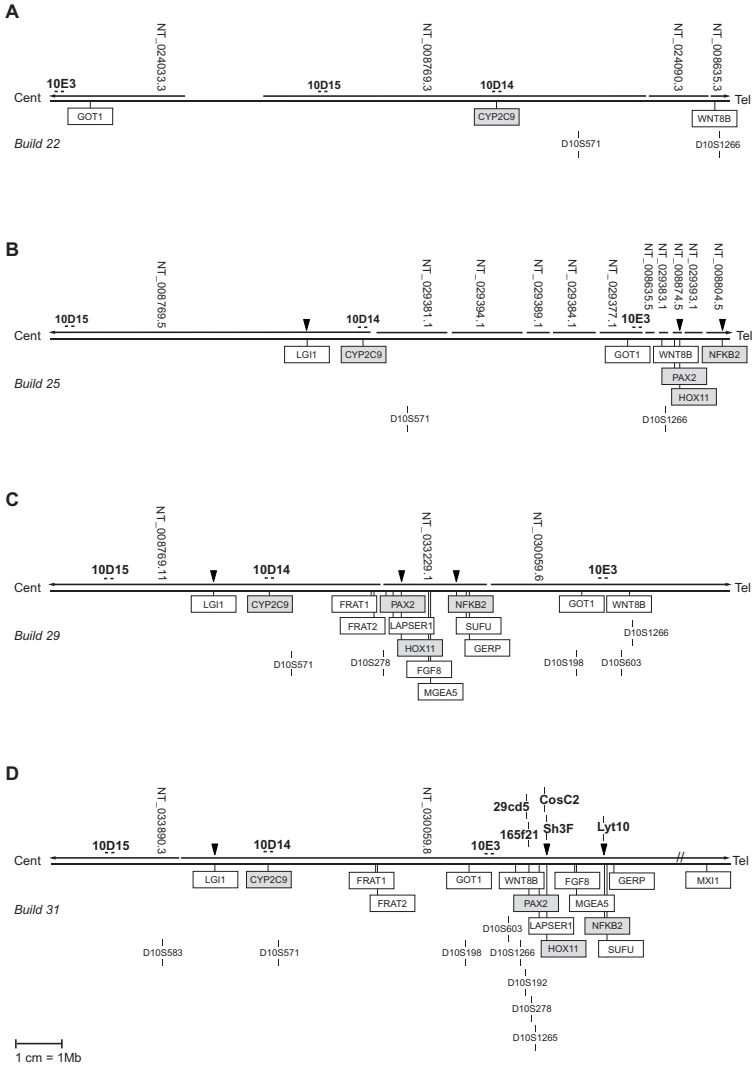

Figure 1

Order and chromosomal orientation of clones mapped by FISH in this study **(D)** aligned with integrated NCBI maps dynamically changing through the time periods April 2001 (Build 22), August 2001 (Build 25), April 2002 (Build 29) and November 2002 (Build 31) **(A-D)**. Genes and sites relevant to reagents used in this study are shown in bold or in grey-filled boxes, and if not marked, were not found in that particular Build. Also indicated are key STS sites common between previously published maps of this region [1–4] (C,D). For A and B, only D10S571, D10S1266, *LGI1*, *GOT1* and *WNT8B* are shown, in addition to markers relevant to the reagents of this study (if found) to illustrate major rearrangements of database contigs within this region through the different NCBI Builds. The locations of 7 additional cancer-related genes are indicated in C and D, with the relative locations of clones used in the present study shown aligned with the recently released Build 31 (D) (see Results for further details). Arrowheads above maps B-D correspond to cancer-related chromosome breakpoint sites associated with disruption of the *LGI1* gene [23,46], *HOX11* [8–13] and *NFKB2/LYT-10* [21,22]. The cancer-related gene *MXI1* [30] maps ~7.5 Mb telomeric of *GERP1*.

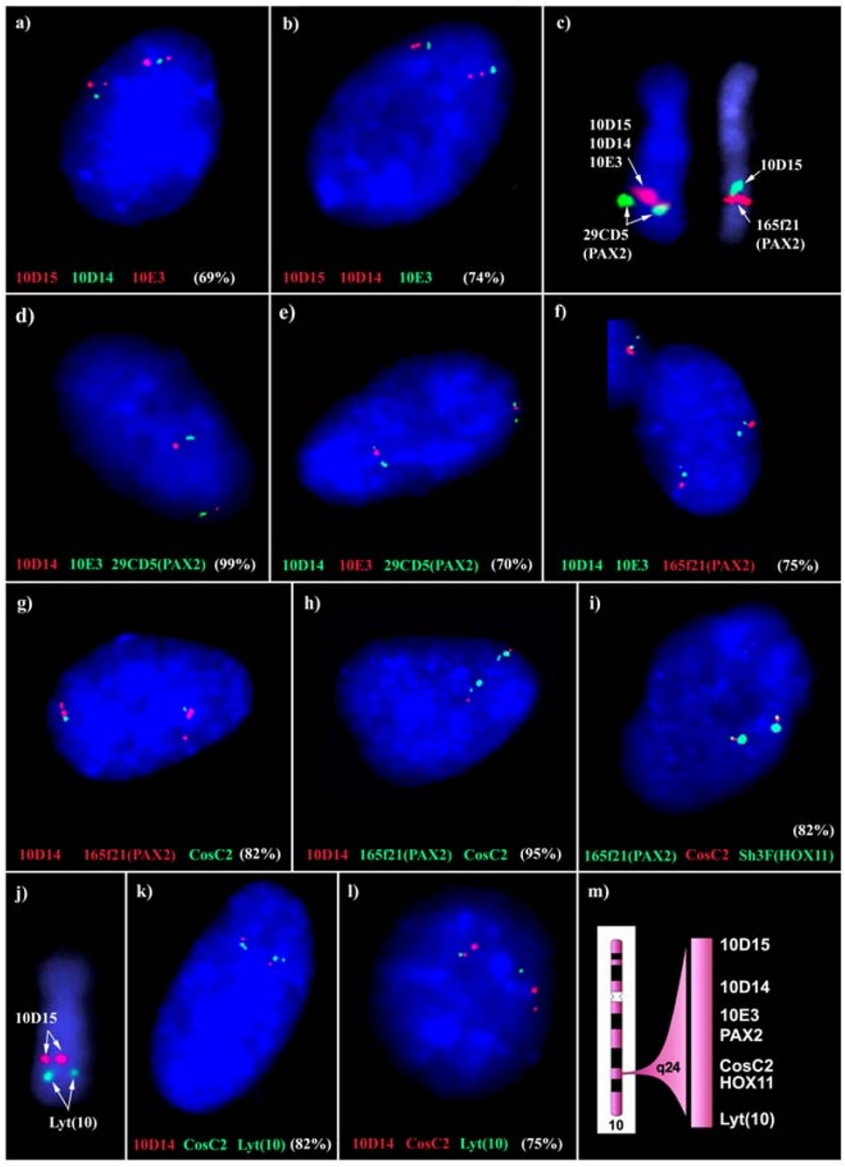

Figure 2
Metaphase **(c,j)** and interphase **(a,b,d-i,k,l)** FISH analysis determines order and relative orientation of selected cancer-related gene probes within 10q24 **(m)**. For interphase figures (a-l), locus identities are indicated in text beneath each representative image, with text color corresponding to the FISH detection color used. Observed frequencies (%) of the probe orders shown are also indicated. Note that the triangular pattern of probes visible on one homologue in a) was classified ambiguous.

Table 1: Order and Frequency of Probe Signal Patterns on Interphase Nuclei after FISH

Probe Combination (Detection Color[1])			Signal Order [No. scored (%)]			
			Red-Gr-Red	Red-Red-Gr	Red-Gr-Gr	Gr-Red-Gr
10D15[b](R)	+ 10D14[d] (Gr)	+ 10E3[b] (R)	38 (69%)	17 (31%)		
10D15[b](R)	+ 10D14[b] (R)	+ 10E3[d] (Gr)	23 (26%)	66 (74%)		
10D14[b] (R)	+ 10E3[d] (Gr)	+ 29CD5 (*PAX2*)[d] (Gr)			75 (99%)	1 (1%)
10D14[d] (Gr)	+ 10E3[b] (R)	+ 29CD5 (*PAX2*)[d] (Gr)			25 (30%)	58 (70%)
10D14[d] (Gr)	+ 10E3[d] (Gr)	+ 165f21 (*PAX2*)[b] (R)			67 (75%)	22 (25%)
10D14[b] (R)	+ 165f21 (*PAX2*)[b] (R)	+ CosC2[d] (Gr)	13 (18%)	61 (82%)		
10D14[b] (R)	+ 165f21 (*PAX2*)[d] (Gr)	+ CosC2[d] (Gr)			79 (95%)	4 (5%)
165f21 (*PAX2*)[d] (Gr)	+ CosC2[b] (R)	+ λSh3F (*HOX11*)[d] (Gr)			7 (18%)	32 (82%)
10D14[b] (R)	+ CosC2[d] (Gr)	+ λ*lyt*-10 (*LYT-10*)[d] (Gr)			76 (82%)	17 (18%)
10D14[b] (R)	+ CosC2[b] (R)	+ λ*lyt*-10 (*LYT-10*)[d] (Gr)	22 (25%)	67 (75%)		

[1]R, red; Gr, Green; [b] Biotin labelled. [d] Digoxygenin labelled. Probe combinations represented correspond to Figures 2a,2b,2d,2e,2f,2g,2h,2i,2k and 2l, respectively.

BAC clones 10E3, 10D14 and 10D15 were each first hybridized to normal metaphase chromosomes and confirmed to map to 10q24 (data not shown). Interphase FISH experiments subsequently revealed the clone order 10D15-10D14-10E3 (Table 1, Figure 2a,2b). The chromosomal orientation of this map was determined when the three pooled biotinylated BAC clones were shown to map centromeric of the digoxygenylated YAC clone 29CD5 (*PAX2*) on the majority of metaphase chromosomes 10 analyzed (Figure 2c, left), and when BAC 10D15 was similarly shown to map centromeric of BAC 165f21 (*PAX2*) (Figure 2c, right). The final centromere-telomere orientation of the BAC clones relative to *PAX2* was established when BACs 10E3 and 10D14 were hybridized in combination with YAC 29CD5 (*PAX2*) or BAC 165f21 (*PAX2*) to interphase nuclei in a series of three different experiments (Table 1, Figure 2d,2e,2f). From this combined data we concluded the preliminary map order centromere-10D15-10D14-10E3-29CD5/165f21/*PAX2*-telomere.

The cosmid C2 (CosC2), reported to contain the HPV6a viral integration site HPV6AI1[42], was next mapped with respect to 10D14 and BAC 165f21(*PAX2*) (Table 1, Figure 2g,2h), indicating the order centromere-10D14-165f21(*PAX2*)-CosC2-telomere (Figure 2m). *HOX11* was shown to map close and immediately telomeric of CosC2 when the λSh3F probe (green) was pooled with BAC 165f21 (green) and CosC2 (red), and hybridized to interphase nuclei. This conclusion was based on the predominant green-red-green signal order for this experiment (Table 1, Figure 2i), the already established centromeric location of *PAX2* relative to CosC2 (Figure 2g,2h), and the smaller size of the λSh3F (*HOX11*) probe and signal (Figure 2i). We note that three cDNA fragments (EMBL:HSAPTB7, EBML:HSAPTL12, EMBL:HSAPTF3) have been isolated from CosC2 and sequenced (NCBI Accession Nos Y11608, Y11609, and Y11610) (Kahn et al, unpublished). Consistent with the above interphase FISH results, BLASTN and Map Viewer http://www.ncbi.nlm.nih.gov/mapview/map_search.cgi? analysis confirmed that all of these cDNA fragments map immediately centromeric of *HOX11* in NCBI Build 31.

The *NFKB2*/*LYT-10* locus represented by the probe λ*lyt*-10 mapped telomeric of 10D14 and CosC2 in two interphase experiments, with the second experiment alternating the CosC2 probe label (Table 1, Figure 2k,2l,2m). A final hybridization of pooled biotinylated and digoxygenylated λ*lyt*-10 probe (yellow) with λPAX2 (red) and λSh3F (*HOX11*) (green) to interphase nuclei determined the order red-green-yellow on 24 of 32 (75%) chromosomes analyzed (data not shown), and confirmed that *NFKB2*/*LYT-10* mapped telomeric of *HOX11*.

The final overall map orientation was confirmed when λ*lyt*-10 (green) was shown to hybridize telomeric of BAC 10D15 (red) (Figure 2j) on metaphase chromosomes, and although not measured statistically, the distance separating 10D15 and λ*lyt*-10 was visibly greater than that which separates 10D15 and BAC 165f21 (*PAX2*) (compare Figure 2c,2j). From these metaphase and interphase FISH studies, we determined the following probe (gene) order within 10q24: centromere-10D15-10D14-10E3-YAC29CD5/BAC165f21(*PAX2*)-CosC2-λSh3F(*HOX11*)-λ*lyt*-10 (*NFKB2*) -telomere (Figure 1d, 2m).

Chromosome 10 clone CosC2 does not contain the human papillomavirus integration site HPV6AI1 which instead maps to chromosome 14

The close proximity of CosC2 and λSh3F (*HOX11*) probes, indicated by a high percentage of overlapping red and green signals (Figure 2i and data not shown), was

noteworthy in this analysis and suggested that the HPV6AI1 integration site (CosC2) maps closely centromeric and probably <200 kb of *HOX11* [43,44]. However, genomic database investigations indicated that the 2746 bp of genomic sequence available across HPV6AI1 (NCBI Accession No_X77607; [42]), and that was originally reported to derive from a *Bam*HI-*Bgl*II subclone of CosC2, is not tightly integrated within 10q24 contigs of the genomic databases (eg. NCBI Map View, Build 31, November, 2002), but instead finds significant, if disrupted, homology across nts 1..2341 (98%) and 2334..2735 (94%) to chromosome 14, at the q13.3-q21.1 band interface (NCBI Accession No NT_026437.9, Build 31) (Figure 3c). Restriction digests of CosC2 released fragment sizes consistent with reported features of that clone [42] (data not shown), and internal Alu-specific primers A51 (forward) and Sb2ins2 (reverse) confirmed the integrity of CosC2 DNA (Figure 3a, left panel, lanes 4–6). However, three PCR primer pairs that were designed to distinguish closely homologous chromosome 14 sequences from those theoretically on 10q24 (Table 2) failed to amplify products from CosC2 under relaxed primer annealing conditions (52°C, 2 mM Mg++) (Figure 3a, right panel, lanes 4–6), but did so from control genomic DNA (Figure 3a, right panel, lanes 1–3). Primer pair A (HPV6apr1/HPV6aRev) amplifies a 615 bp product common to both X77607 and homologous chromosome 14 sequence (Figure 3a,3c). Primer pairs B (Chr14gapF/Chr14gapR) and C (Chr14endF/Chr14endR) were designed to amplify 535 bp and 699 bp products specific to chromosome 14 sequence as determined by genomic database comparisons (Figure 3a,3c). When hybridized to a Southern-blotted human chromosome-specific somatic cell hybrid panel, the 615 bp fragment showed positive signals only in the control and chromosome 14-specific lanes (Figure 3b). From these studies we conclude that CosC2 does not contain the 2746 bp viral integration site HPV6AI1 of NCBI Accession X77607, but that this site instead maps to the chromosome band 14q13.3-q21.1 interface. We are unable to explain the 209 bp of sequence that is present on chromosome 14q but not in X77607 (Figure 3c). The chromosome 14 "insertion" occurs within a L1PREC2 nontransposable repeat element, and may correspond to an insertion/deletion polymorphism although sequence artifact cannot be excluded.

BAC End Sequencing Allows Integration of FISH Results into Genomic 10q24 Map

To facilitate the orientation and relative locations of probes used for FISH studies, T7-primed genomic end-sequences of BAC clones 10D14, 10D15 and 10E3 were submitted to BLASTN after identification of repetitive sequences using CENSOR. In the sequence release of Build 31 (November 2002), a 520 bp end-sequence of 10D15 showed 95% homology across nucleotides (nts) 11626039–11626469 of NCBI contig NT_033890.3 (Figure 1d), consistent with its most centromeric location in our study (Figure 1d). A 700 bp end-sequence of 10D14 showed 98% homology across nts 8367245–8367938 towards the telomeric end of the same contig as 10D15 in Build 29, mapping ~650 bp upstream of the 5' start of the cytochrome P4502C9 (*CYP2C9*) gene (Figure 1c and data not shown). In Build 31, end-sequences of 10D15 and 10D14 (NT_030059.8, nts 1961641–1962337) have been mapped to different juxtaposing contigs. The spatial and chromosomal orientation of 10D15 and 10D14 through these two Builds is, however, consistent with our FISH interphase mapping results, which show that *CYP2C9* maps centromeric of the *PAX2/HOX11/NFKB2* region (Figure 1d). Finally, a 650 bp end-sequence of 10E3 showed 99% homology across nts 12098591–12097943 of contig NT_030059.6 in Build 29 (Figure 1c). This location is inconsistent with the visibly centromeric location and closer proximity of 10E3 to *PAX2* (YAC 29CD5/BAC 165f21) in interphase FISH experiments (Figure 2c,2d,2e), a finding that is more consistent with the relocation in Build 31 of contig NT_030059.8 which contains the 10E3 homologous nts 6881174–6881822 (Figure 1d).

Alignment of BACs 10D14, 10D15 and 10E3 end-sequences against 10q24 contigs of earlier NCBI Builds 22 (April 2001), 25 (August 2001) and 29 (April 2002) graphically reflects the dynamically evolving assembly of contigs, genes and markers within this region (compare Figures 1a,1b,1c). Our FISH interphase mapping and BAC-end sequencing results fitted best into the current NCBI sequence contigs (NCBI Build 31) (Figure 1d), and is also in agreement with the Human Genome Project Working Draft http://genome.ucsc.edu/ described by the International Human Genome Sequencing Consortium [45]. The relative locations of 9 other genes reported to be structurally or functionally implicated in malignancy, including *LGI1* [23,46], *FRAT1* [47], *FRAT2* [48], *WNT8B* [49], *LAPSER1* [32], *FGF8* [50], *MGEA5* [51], *SUFU* [52] and *GERP* (*TRIM8*) [53], the STS markers D10S583, D10S571, D10S198, D10S603, D10S1266, D10S192, D10S278, D10S1265 and the gene *GOT1* were determined by BLASTN comparison of deposited sequences against the NCBI databases (Figure 1c,1d).

Discussion

Using interphase FISH we have determined the relative order of selected cancer-related genes that map within chromosome band 10q24. This analysis, complemented by BAC end-sequencing and genomic database analysis, has also established the chromosomal orientation of NCBI nucleotide contigs that contain these genes, and which span ~11 Mb. The gene and marker order that we have determined is centromere-BAC10D15-BAC10D14/CYP2C9-

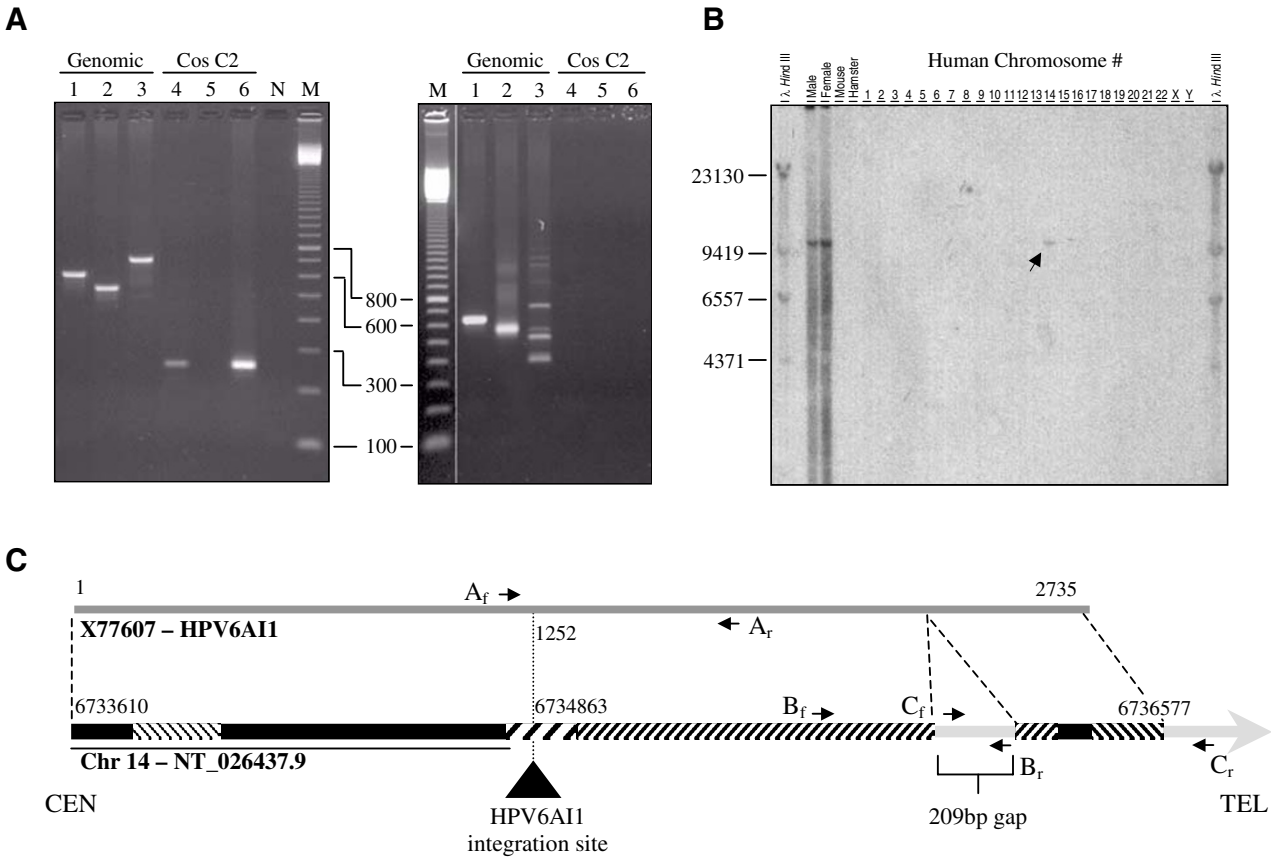

Figure 3

PCR confirms absence of the HPV6AI1 site in the recombinant cosmid clone CosC2. **(A)** Gel electrophoresis of products amplified from human genomic DNA and CosC2 DNA using PCR primer sets A, B and C, and Alu-specific primers (refer Figure 3C, Table 2). In the *left panel*, lanes 1–3 show genomic DNA fragments amplified with primer sets A (615 bp product), B (535 bp product), and C (699 bp product), all at 1.5 mM Mg++ and annealed at 60°C. Lane 4 shows CosC2 DNA amplified with Alu primers A51/Sb2ins2. Lanes 5 and 6 are, respectively, negative (no DNA) and positive genomic DNA controls for this primer set. Lane N is a negative control (no DNA) for primer set A. In the *right panel*, lanes 1–3 are as in the left panel except that reactions were at 2 mM Mg++ with annealing at 52°C. Note the presence of additional bands in lane 3 under these relaxed stringency PCR conditions. Lanes 4–6, under the same conditions, show no product from the CosC2 template using the primers sets A, B and C respectively. In both left and right panels, M is a 100 bp molecular weight reference ladder. (**B**) Somatic cell hybrid panel showing *Pst*I fragments of ~9.5 kb detected in control male and female genomic DNA lanes, and in the chromosome 14 specific lane (arrow) after hybridization with the ^{32}P-dCTP labeled 615 bp fragment amplified using primer set A. λ *Hind*III fragment sizes are indicated to the left of the panel. (**C**) Alignment of the published sequence X77607 with contig NT_026437.9 from chromosome (chr) 14. In the lower figure, the thin grey line corresponds to chr 14 sequence, and thicker solid (repeat-free) or hatched boxes correspond to regions that have overlapping homology with X77607. Repeat sequences identified using CENSOR are shown as diagonal hatched regions corresponding to CHESHIRE_B (narrow downward), LIPB4 (wide upward), L1PREC2 (narrow upward) and THE1B (wide downward). Flanking nt sequence locations are indicated for each contig, as is the location of the HPV6AI1 integration site. Locations of primer pairs A-C are marked by forward (f) and reverse (r) arrows. The bracketed region marks 209 bp of chr 14 sequence not present in X77607.

Table 2: PCR primer sequences and reaction conditions used to verify localization of *HPV6AI1*

Primer ID	Locus	Primer Sequence (5' > 3')[a]	Annealing Temp (°C)	Mg++ (mM)	Primer Pair ID[b]
HPV6apr1	HPV6AI1[c]	F-TTATAGATTCGGGGGTACACACGTAG	60	1.5	A
HPV6aRev	HPV6AI1[c]	R-AGCAGAGAAAAGGAATGCCGATAT	60	1.5	
Chr14gapF	14q13[d]	F-TCTTGTTAAATTGTTTGAGTTCC	60	1.5	B
Chr14gapR	14q13[d]	R-CTATTCTAATCAAAACAGCATGG	60	1.5	
Chr14endF	14q13[d]	F-TATTGAATAGAGAGTCCTTTCCC	60	1.5	C
Chr14endR	14q13[d]	R-TAAACCTCATCTTGAATTGTAGC	60	1.5	
A51	Alu[e]	F-GGCGCGGTGGCTCACG	65	1.5	Alu
Sb2ins2	Alu Sb2[f]	R-GGCCGGACTGCGGACTGCA	65	1.5	

a, F = forward, R = reverse; b, as represented in Figure 3; c,d derived from NCBI Accession No X77607 and NT_025892.8, respectively; e,f derived from Alu-repeat consensus and AluYb8 (Sb2) subfamily-specific consensus sequences, respectively (Labuda et al, unpublished).

BAC10E3-*PAX2*-CosC2-*HOX11*-*NFKB2/LYT-10*-telomere. The order of genes and markers on our map differs from the NCBI release of Build 29, and is more consistent with previous NCBI releases including Build 25, with the June 2002 freeze of the UCSC Human Genome Project Working Draft http://genome.ucsc.edu/ and with the more recently released NCBI Build 31.

There have been several published studies designed to clarify the physical map across 10q24 [1], although none have specifically focussed on the order and orientation of cancer-related genes or sites of inter- and intra-chromosomal rearrangement involving this region. In one of these reports, Gray et al applied a combination of metaphase FISH (to confirm 10q24 map location) and PCR amplification of microsatellite, STS and other known gene markers to the analysis of a series of overlapping YACs spanning ~15 Mb of DNA [1]. Of particular interest, Gray et al noted a high frequency of rearranged YACs (4/5 analysed) distal to D10S574 and incorporating the *GOT1*, *WNT8B* and *PAX2* gene cluster. That feature, combined with the inability to isolate YAC clones immediately telomeric of this region, a known BrdU-inducible fragile site in 10q24-q25, and chromosome translocation breakpoint clusters associated with ALL and other lymphoproliferative neoplasms is suggestive of inherent instability of this chromosomal segment [1]. To date, although chromosomal imbalances involving this region are prevalent across a wide variety of different cancer subtypes, the genomic basis for this instability has yet to be explained.

In the separate study of Nikali and colleagues, which was designed to refine the map location of the IOSCA locus at 10q24, a similar map configuration was derived [2]. For this study, radiation hybrid analysis was used to determine the order of selected microsatellite and other known STS or gene markers, including *PAX2*, across a >500 kb region between D10S198 and D10S222 [2]. Fibre-FISH was also used to confirm the order and orientation of selected clones within the IOSCA region but did not confirm chromosomal orientation of the contig under study [2].

Neither of the above two studies, nor others reported subsequently [4,54–56], have provided unequivocal evidence of the centromere-telomere orientation of *PAX2*, *HOX11* and *NFKB2/LYT-10* within the 10q24 region that we have targeted. Nor do they include analyses that convincingly demonstrate the relative location of these and other cancer-related genes across this region. Most published investigations to date have used YAC clones and microsatellite analysis to map the 10q24 region, or have referenced maps constructed with YACs. However, the reported propensity for YACs derived from this region to undergo internal rearrangement and deletions may have contributed to map inconsistencies. The information we have presented is based mostly on smaller insert BAC, cosmid and bacteriophage clones. Our clarification of the 10q24 physical map is complementary to the International Human Genome Sequencing Consortium BAC-derived assemblies hosted by the NCBI, and will enable more precise mapping of chromosome translocation breakpoints or other structural rearrangements associated with malignant and nonmalignant disease conditions.

Our FISH studies show that the cosmid clone CosC2 maps close, centromeric and upstream of the homeobox gene *HOX11*. This finding was of interest because CosC2 reportedly contains the HPV6a viral integration site HPV6AI1 previously associated with an infiltrating squamous cell carcinoma of the tonsil [42], and suggested that deregulation of *HOX11* by the integration process may have been implicated in this malignancy. However, genomic database analysis of sequences that did not derive specifically from the germline CosC2 insert but which directly flank the previously described HPV6a integration site indicates that HPV6AI1 maps not to 10q24 but to the interface of chromosome band 14q13.3-q21.1. Further database analysis showed that HPV6a integration occurred within a L1PB4 nontransposable repeat, and be-

tween the predicted coding domains of FLJ30803 and LOC122529 (data not shown). This location was confirmed by subsequent PCR and somatic cell hybrid investigations. We presume that the cosmid clone C2 was spuriously selected during the original screening process, for which a probe derived from the sequenced region X77607 was used [42].

The human papillomaviruses (HPVs) are a diverse family that type-specifically infects distinct subsets of epithelial cells. The HPV genome persists as an extrachromosomal episome in non- or premalignant tissues, whereas in invasive cancers, the viral DNA typically integrates into the host genome. This event has been shown to increase stability of HPV16 E6 and E7 mRNAs [57]. Recent evidence suggests that HPV integration sites associated with malignancy are distributed widely across the human genome rather than preferentially localized [58–60]. However, there is a recognized propensity for HPV DNA integration to occur in or near fragile sites, translocation breakpoint sites, oncogenes or the coding regions of as yet poorly characterized genes that may have relevance to cancer progression [59–65]. Although HPV6AI1 does not appear to interrupt a coding domain, it is of interest that the HPV6AI1 site falls within a repeat element and close to a possible insertion/deletion polymorphism site on chromosome 14. These findings are consistent with the highly recombinogenic/unstable regions in which papillomavirus integrations are predicted to occur.

Previously published studies of the HPV6a integration site we have relocalized showed that the corresponding normal allele was not present in the originally characterized tonsillar carcinoma cells [42]. Rearrangements in the region of the HPV6a integration site were also implicated by Southern blot analysis of a limited number of other tumors, including 2 of 25 genital condylomas, and 2 (1 tonsillar, 1 hypopharnyx) of 7 head and neck tumors tested [42]. Together, these findings were suggestive that the HPV6a genome had disrupted a novel cancer-related gene or gene regulatory region at 10q24. However, analyses reported here indicate that this site instead maps to 14q13.3-q21.1, and that loci FLJ30803 and LOC122529 may be two such candidate genes. Further investigations of the chromosome 14 integration site are necessary to verify its functional relevance to HPV-related malignancies.

Conclusions

We have applied chromosome and interphase fluorescent in situ hybridization (FISH), BAC end-sequencing, PCR and genome database analysis to map the order and chromosomal orientation of selected cancer-related genes within chromosome band 10q24, and the human papillomavirus Type 6a (HPV6a) viral integration site HPV6AI1. The 10q24 region is already known to harbor several well studied cancer-related genes, but published cytogenetic, comparative genomic hybridization, allelotyping and other molecular studies suggest that yet to be identified genes relevant to cancer initiation and progression map within this domain. Towards this end it is vital to establish a definitive genetic map of this region, which to date has shown considerable volatility through time in published works of scientific journals, within different builds of the same international genomic database, and across the differently constructed databases. This volatility has proved an ongoing frustration for positional cloning efforts such as those we are pursuing, and it is for this reason that we found the present study necessary. We describe new data that confirms the order CEN-*CYP2C9-PAX2-HOX11-NFKB2*-TEL. This finding resolves the physical arrangement of larger DNA sequence contigs containing these and at least 10 other genes which have so far been implicated in different cancer subtypes. Furthermore, our studies show that the viral integration site HPV6AI1 does not map within 10q24, but at a different chromosomal site, namely at the interface of chromosome bands 14q13.3-q21.1. This is a significant finding and important to report because the HPV6AI1 integration site, originally isolated from a tonsillar carcinoma, was shown to be rearranged in other HPV6a-related malignancies, including 2 of 25 genital condylomas, and 2 of 7 head and neck tumors tested (Kahn et al, 1994, *Cancer Res*. **54**: 1305–1312). Our finding shifts the focus of this genomic interest from 10q24 to a site on chromosome 14 that may potentially harbor a gene with an as yet undetermined role in the etiology of carcinogenesis.

Methods

Genomic clones

Recombinant YAC, BAC and bacteriophage lambda clones were used to determine the relative order and orientation of the *CYP2C9*, *NFKB2/LYT-10*, *HOX11* and *PAX2* gene loci, and the HPV6AI1 integration site. BAC clones 10D15, 10D14 and 10E3 were selected from the Cedars-Sinai Medical Center Genomic Reagents Resource database http://www.csmc.edu/genetics/korenberg/int-bac-sts.html based on their preliminary map location at 10q24 [66]. BAC clone 165f21, which contains the *PAX2* gene, was kindly gifted by Dr K. Nikali (National Public Health Institute, Helsinki, Finland), and YAC clone 29CD5 was isolated from the ICRF YAC library using PCR primers specific for *PAX2* (Eccles et al, unpublished). Genomic lambda (λ) clones of *PAX2* (λPAX2) and *HOX11* (λSh3F) were also isolated from a genomic liver library constructed in λGem-11 (Promega, Madison, WI). Radioactively labelled probes used to screen the λ library as previously described were pG3a [67] and Sh3F [9] for *PAX2* and *HOX11*, respectively. The phage clone λ*lyt*-10 contains a 12 kb genomic fragment including the entire

NFKB2/LYT-10 coding sequence [68]. The previously described cosmid clone CosC2 is reported to contain the viral integration site HPV6AI1 [42].

Fluorescent In Situ Hybridization (FISH)

Procedures used, including preparation of metaphase or interphase nuclei from peripheral blood or G1 fibroblasts, slide pre-treatment, probe labeling with biotin or digoxygenin, repeat suppression, hybridization parameters, and single- or two-color immuno-fluorescent detection of labeled probes, were essentially as described [69,70]. Fluorescent images from metaphase or interphase cells were captured at selective bandwidths to computer using a Leitz Aristoplan microscope fitted with a Photometrics KAF1400 CCD camera and QUIPS Smartcapture software (version 1.3; Vysis Inc, Downers Grove, IL, USA). Probes were mapped precisely to chromosome bands in metaphase cells, or relative to each other in interphase cells, using color-joined DAPI, FITC and Texas Red images, and QUIPS CGH/Karyotyping software (version 3.0.2). To avoid damaged cells, metaphase and G1 interphase nuclei were initially selected for analysis under a DAPI-selective filter. G1 interphase nuclei were subsequently scored only if red or green signals corresponding to all probes hybridized were distinguishable on both homologues.

Polymerase Chain Reaction (PCR)

Primer sequences designed to amplify HPV6AI1, the homologous region on chromosome 14q and a control internal Alu-specific 260 bp fragment are as listed in Table 2. PCR reactions contained 100 ng of template DNA, 200 μM dNTPs, 500 nM of each primer, reaction buffer (50 mM KCl, 10 mM Tris pH 8.3, 1.5 or 2.0 mM $MgCl_2$) and 0.5 units Platinum™ Taq DNA polymerase (Life Technologies). Following 30 cycles of amplification [denaturation 95°C, 30 sec; annealing (refer Table 2), 30 sec, extension 72°C, 30 sec], the PCR products were electrophoresed in 1.5% agarose gels and visualized by ethidium bromide staining. Products were transferred to Hybond N^+ nylon membrane (Amersham, Buckinghamshire, UK) and hybridized with Rediprime random-prime ^{32}P-labeled probes (Amersham) following the manufacturer's instructions. Control human genomic DNA for PCR studies was extracted from healthy subjects using methods previously described [71].

Somatic Cell Hybrid Analysis

A Southern blot containing *Pst*I digested genomic DNA from a human-rodent somatic cell hybrid panel was obtained from Oncor (Gaithersburg, MD) and hybridized with ^{32}P-dCTP-labeled DNA fragments as outlined above.

BAC DNA End-Sequencing

End-sequencing of BAC clones 10D14, 10D15 and 10E3 (cloning vector pBAC108L; Shizuya et al., 1992) was performed using ThermoSequenase (Amersham) and a universal T7 IRD41-labeled primer (MWG Biotech, Germany) essentially according to the manufacturers recommendations. Reactions were separated on a LICOR 4000L semi-automated DNA sequencer, and nucleotide sequences subsequently submitted to BLASTN for homology determination.

Genomic Database Resources

Genomic database resources utilized early in this study include the GTC Integrated STS Map http://www.genomecorp.com; http://ihg.gsf.de/chr10/report_text.html#parti, the Southhampton Integrated Map ftp://cedar.genetics.soton.ac.uk/pub/chrom10/gmap, the Whitehead YAC contig WC10.8 http://www-genome.wi.mit.edu/cgi-bin/contig/lookup_contig and the NCBI GeneMap 98 http://www.ncbi.nlm.nih.gov/genemap98/map.cgi?CHR=10. The International Human Genome Sequencing Consortium assemblies of the Human Genome sequence hosted by the NCBI http://www.ncbi.nlm.nih.gov/genome/guide/human/release_notes.html[43], including NCBI MapViewer Builds 22, 25, 29 and 31 corresponding to releases of April 2001, August 2001, April 2002, and November 2002 respectively, were additional sources of data complementary to our findings presented in Figure 1. Repeat sequences were identified within the BAC end-sequences and in the HPV6AI1 integration site using CENSOR http://www.girinst.org/Censor_Server.html prior to BLASTN homology searches http://ncbi.nlm.nih.gov/BLAST.

Authors contributions

SG performed most of the FISH experiments, contributed to experimental design, collected and collated most of the final data, and contributed significantly to the final draft of the manuscript including preparation of the final tables and figures; MMcD assisted with FISH experiments including hybridisations and analysis; XNC and JK provided BAC clones 10D15, 10D14 and 10E3 and offered guidance to the culture and purification of DNA from these clones; AN provided the λ*lyt*-10 clone; TK provided the cosmid clone CosC2, and assisted with final interpretation of the revised HPV6a viral integration site findings; ME provided the YAC clone 29CD5, purifed DNA from λPAX2 and λSh3F, and sourced the BAC clone 165f21; CM first conceptualised the study, participated in its design and coordination, and assisted with preparation of the final manuscript. All authors have read and approved the final manuscript.

Acknowledgments

We thank Drs Ruth Spearing, Peter Ganly and Chris Atkinson for support that has enabled the completion of this study, Drs M Kennedy and T Rabbits for the *H0X11* cDNA clone λSh3F, Dr Kaisu Nikali for the *PAX2* BAC and Dr Damian Labuda who provided the AluYb8-specific A51 and Sb2ins2 primer sequences. This work was supported by the Cancer Society of New

Zealand, the W.H. Travis Trust, the Robert McClelland Trust, and the New Zealand Leukaemia and Blood Foundation.

References

1. Gray IC, Fallowfield J, Ford S, Nobile C, Volpi EV and Spurr NK **An integrated physical and genetic map spanning chromosome band 10q24.** *Genomics* 1997, **43:**85-88
2. Nikali K, Isosomppi J, Lonnqvist T, Mao JI, Suomalainen A and Peltonen L **Toward cloning of a novel ataxia gene: refined assignment and physical map of the IOSCA locus (SCA8) on 10q24.** *Genomics* 1997, **39:**185-191
3. Ford S, Gray IC and Spurr NK **Rearrangement of the long arm of chromosome 10 in the prostate adenocarcinoma cell line LNCaP.** *Cancer Genet Cytogenet* 1998, **102:**6-11
4. Nobile C, Manca A, Pisano M, Angius A, Gray IC and Spurr NK **A refined physical and EST map spanning 7.4 Mb of 10q24, a region involved in neurological disorders.** *Mamm Genome* 1998, **9:**835-837
5. Dear TN, Sanchez-Garcia I and Rabbitts TH **The HOX11 gene encodes a DNA-binding nuclear transcription factor belonging to a distinct family of homeobox genes.** *Proc Natl Acad Sci U S A* 1993, **90:**4431-4435
6. Roberts CW, Shutter JR and Korsmeyer SJ **Hox11 controls the genesis of the spleen.** *Nature* 1994, **368:**747-749
7. Dear TN, Colledge WH, Carlton MB, Lavenir I, Larson T, Smith AJ, Warren AJ, Evans MJ, Sofroniew MV and Rabbitts TH **The Hox11 gene is essential for cell survival during spleen development.** *Development* 1995, **121:**2909-2915
8. Hatano M, Roberts CW, Minden M, Crist WM and Korsmeyer SJ **Deregulation of a homeobox gene, HOX11, by the t(10;14) in T cell leukemia.** *Science* 1991, **253:**79-82
9. Kennedy MA, Gonzalez-Sarmiento R, Kees UR, Lampert F, Dear N, Boehm T and Rabbitts TH **HOX11, a homeobox-containing T-cell oncogene on human chromosome 10q24.** *Proc Natl Acad Sci U S A* 1991, **88:**8900-8904
10. Salvati PD, Ranford PR, Ford J and Kees UR **HOX11 expression in pediatric acute lymphoblastic leukemia is associated with T-cell phenotype.** *Oncogene* 1995, **11:**1333-1338
11. Salvati PD, Watt PM, Thomas WR and Kees UR **Molecular characterization of a complex chromosomal translocation breakpoint t(10;14) including the HOX11 oncogene locus.** *Leukemia* 1999, **13:**975-979
12. Watt PM, Kumar R, Kees UR, Salvati PD, Thomas WR, Ranford PR and Ford J **Promoter demethylation accompanies reactivation of the HOX11 proto-oncogene in leukemia.** *Genes Chromosomes Cancer* 2000, **29:**371-377
13. Kahl C, Gesk S, Harder L, Harbott J, French L, Deloukas P, Grote W, Schlegelberger B and Siebert R **Detection of translocations involving the HOX11/TCL3-locus in 10q24 by interphase fluorescence in situ hybridization.** *Cancer Genet Cytogenet* 2001, **129:**80-804
14. Porteous S, Torban E, Cho NP, Cunliffe H, Chua L, McNoe L, Ward T, Souza C, Gus P and Giugliani R **Primary renal hypoplasia in humans and mice with PAX2 mutations: evidence of increased apoptosis in fetal kidneys of Pax2(1Neu) +/- mutant mice.** *Hum Mol Genet* 2000, **9:**1-11
15. Khoubehi B, Kessling AM, Adshead JM, Smith GL, Smith RD and Ogden CW **Expression of the developmental and oncogenic PAX2 gene in human prostate cancer.** *J Urol* 2001, **165:**2115-2120
16. Silberstein GB, Dressler GR and Van Horn K **Expression of the PAX2 oncogene in human breast cancer and its role in progesterone-dependent mammary growth.** *Oncogene* 2002, **21:**1009-1016
17. Dressler GR and Woolf AS **Pax2 in development and renal disease.** *Int J Dev Biol* 1999, **43:**463-468
18. Eccles MR, He S, Legge M, Kumar R, Fox J, Zhou C, French M and Tsai RW **PAX genes in development and disease: the role of PAX2 in urogenital tract development.** *Int J Dev Biol* 2002, **46:**535-544
19. Chen F, Castranova V, Shi X and Demers LM **New insights into the role of nuclear factor-kappaB, a ubiquitous transcription factor in the initiation of diseases.** *Clin Chem* 1999, **45:**7-17
20. Karin M, Cao Y, Greten FR and Li ZW **NF-kappaB in cancer: from innocent bystander to major culprit.** *Nat Rev Cancer* 2002, **2:**301-310
21. Neri A, Fracchiolla NS, Migliazza A, Trecca D and Lombardi L **The involvement of the candidate proto-oncogene NFKB2/lyt-10 in lymphoid malignancies.** *Leuk Lymphoma* 1996, **23:**43-48
22. Kim KE, Gu C, Thakur S, Vieira E, Lin JC and Rabson AB **Transcriptional regulatory effects of lymphoma-associated NFKB2/lyt10 protooncogenes.** *Oncogene* 2000, **19:**1334-1345
23. Chernova OB, Somerville RP and Cowell JK **A novel gene, LGI1, from 10q24 is rearranged and downregulated in malignant brain tumors.** *Oncogene* 1998, **17:**2873-2881
24. Morante-Redolat JM, Gorostidi-Pagola A, Piquer-Sirerol S, Saenz A, Poza JJ, Galan J, Gesk S, Sarafidou T, Mautner VF and Binelli S **Mutations in the LGI1/Epitempin gene on 10q24 cause autosomal dominant lateral temporal epilepsy.** *Hum Mol Genet* 2002, **11:**1119-1128
25. Kalachikov S, Evgrafov O, Ross B, Winawer M, Barker-Cummings C, Martinelli Boneschi F, Choi C, Morozov P, Das K and Teplitskaya E **Mutations in LGI1 cause autosomal-dominant partial epilepsy with auditory features.** *Nat Genet* 2002, **30:**335-341
26. Virmani AK, Fong KM, Kodagoda D, McIntire D, Hung J, Tonk V, Minna JD and Gazdar AF **Allelotyping demonstrates common and distinct patterns of chromosomal loss in human lung cancer types.** *Genes Chromosomes Cancer* 1998, **21:**308-319
27. Zhou X, Kemp BL, Khuri FR, Liu D, Lee JJ, Wu W, Hong WK and Mao L **Prognostic implication of microsatellite alteration profiles in early-stage non-small cell lung cancer.** *Clinical Cancer Research* 2000, **6:**559-565
28. Lundgren R, Mandahl N, Heim S, Limon J, Henrikson H and Mitelman F **Cytogenetic analysis of 57 primary prostatic adenocarcinomas.** *Genes Chromosomes Cancer* 1992, **4:**16-24
29. Gray IC, Phillips SM, Lee SJ, Neoptolemos JP, Weissenbach J and Spurr NK **Loss of the chromosomal region 10q23-25 in prostate cancer.** *Cancer Res* 1995, **55:**4800-4803
30. Prochownik EV, Eagle Grove L, Deubler D, Zhu XL, Stephenson RA, Rohr LR, Yin X and Brothman AR **Commonly occurring loss and mutation of the MXI1 gene in prostate cancer.** *Genes Chromosomes Cancer* 1998, **22:**295-304
31. Alers JC, Rochat J, Krijtenburg PJ, Hop WC, Kranse R, Rosenberg C, Tanke HJ, Schroder FH and van Dekken H **Identification of genetic markers for prostatic cancer progression.** *Laboratory Investigation* 2000, **80:**931-942
32. Cabeza-Arvelaiz Y, Thompson TC, Sepulveda JL and Chinault AC **LAPSER1: a novel candidate tumor suppressor gene from 10q24.3.** *Oncogene* 2001, **20:**6707-6717
33. Leube B, Drechsler M, Muhlmann K, Schafer R, Schulz WA, Santourlidis S, Anastasiadis A, Ackermann R, Visakorpi T and Muller W **Refined mapping of allele loss at chromosome 10q23-26 in prostate cancer.** *Prostate* 2002, **50:**135-144
34. Cappellen D, Gil Diez de Medina S, Chopin D, Thiery JP and Radvanyi F **Frequent loss of heterozygosity on chromosome 10q in muscle-invasive transitional cell carcinomas of the bladder.** *Oncogene* 1997, **14:**3059-3066
35. Simon R, Burger H, Brinkschmidt C, Bocker W, Hertle L and Terpe HJ **Chromosomal aberrations associated with invasion in papillary superficial bladder cancer.** *J Pathol* 1998, **185:**345-351
36. Richter J, Wagner U, Schraml P, Maurer R, Alund G, Knonagel H, Moch H, Mihatsch MJ, Gasser TC and Sauter G **Chromosomal imbalances are associated with a high risk of progression in early invasive (pT1) urinary bladder cancer.** *Cancer Res* 1999, **59:**5687-5691
37. Parmiter AH, Balaban G, Clark WH Jr and Nowell PC **Possible involvement of the chromosome region 10q24----q26 in early stages of melanocytic neoplasia.** *Cancer Genet Cytogenet* 1988, **30:**313-317
38. Reifenberger J, Knobbe CB, Wolter M, Blaschke B, Schulte KW, Pietsch T, Ruzicka T and Reifenberger G **Molecular genetic analysis of malignant melanomas for aberrations of the WNT signaling pathway genes CTNNB1, APC, ICAT and BTRC.** *Int J Cancer* 2002, **100:**549-556
39. Speaks SL, Sanger WG, Masih AS, Harrington DS, Hess M and Armitage JO **Recurrent abnormalities of chromosome bands 10q23-25 in non-Hodgkin's lymphoma.** *Genes Chromosomes Cancer* 1992, **5:**239-243

40. Scarisbrick JJ, Woolford AJ, Russell-Jones R, Whittaker SJ, Fujiwara Y, Hoon DS, Yamada T, Umeshita K, Gotoh M and Sakon M **Loss of heterozygosity on 10q and microsatellite instability in advanced stages of primary cutaneous T-cell lymphoma and possible association with homozygous deletion of PTEN.** *Blood* 2000, **95:**2937-2942
41. Wilson KS, McKenna RW, Kroft SH, Dawson DB, Ansari Q and Schneider NR **Primary effusion lymphomas exhibit complex and recurrent cytogenetic abnormalities.** *Br J Haematol* 2002, **116:**113-121
42. Kahn T, Turazza E, Ojeda R, Bercovich A, Stremlau A, Lichter P, Poustka A, Grinstein S and zur Hausen H **Integration of human papillomavirus type 6a DNA in a tonsillar carcinoma: chromosomal localization and nucleotide sequence of the genomic target region.** *Cancer Res* 1994, **54:**1305-1312
43. Trask BJ, Massa H, Kenwrick S and Gitschier J **Mapping of human chromosome Xq28 by two-color fluorescence in situ hybridization of DNA sequences to interphase cell nuclei.** *Am J Hum Genet* 1991, **48:**1-15
44. Senger G, Ragoussis J, Trowsdale J and Sheer D **Fine mapping of the human MHC class II region within chromosome band 6p21 and evaluation of probe ordering using interphase fluorescence in situ hybridization.** *Cytogenetics & Cell Genetics* 1993, **64:**49-53
45. IHGS Consortium **Initial sequencing and analysis of the human genome.** *Nature* 2001, **409:**860-921
46. Chernova O and Cowell JK **Molecular definition of chromosome translocations involving 10q24 and 19q13 in human malignant glioma cells.** *Cancer Genet Cytogenet* 1998, **105:**60-68
47. Jonkers J, Korswagen HC, Acton D, Breuer M and Berns A **Activation of a novel proto-oncogene, Frat1, contributes to progression of mouse T-cell lymphomas.** *Embo J* 1997, **16:**441-450
48. Saitoh T, Moriwaki J, Koike J, Takagi A, Miwa T, Shiokawa K and Katoh M **Molecular cloning and characterization of FRAT2, encoding a positive regulator of the WNT signaling pathway.** *Biochemical & Biophysical Research Communications* 2001, **281:**815-820
49. Saitoh T, Mine T and Katoh M **Up-regulation of WNT8B mRNA in human gastric cancer.** *International Journal of Oncology* 2002, **20:**343-348
50. Yoshiura K, Leysens NJ, Chang J, Ward D, Murray JC and Muenke M **Genomic structure, sequence, and mapping of human FGF8 with no evidence for its role in craniosynostosis/limb defect syndromes.** *Am J Med Genet* 1997, **72:**354-362
51. Heckel D, Comtesse N, Brass N, Blin N, Zang KD and Meese E **Novel immunogenic antigen homologous to hyaluronidase in meningioma.** *Hum Mol Genet* 1998, **7:**1859-1872
52. Stone DM, Murone M, Luoh S, Ye W, Armanini MP, Gurney A, Phillips H, Brush J, Goddard A and de Sauvage FJ **Characterization of the human suppressor of fused, a negative regulator of the zinc-finger transcription factor Gli.** *J Cell Sci* 1999, **112:**4437-4448
53. Vincent SR, Kwasnicka DA and Fretier P **A novel RING finger-B box-coiled-coil protein, GERP.** *Biochem Biophys Res Commun* 2000, **279:**482-486
54. Nobile C and Pitzalis S **Expression analysis of 21 transcripts physically anchored within the chromosomal region 10q24 [In Process Citation].** *Genomics* 1999, **62:**86-89
55. Lo Nigro C, Cusano R, Scaranari M, Cinti R, Forabosco P, Morra VB, De Michele G, Santoro L, Davies S and Hurst J **A refined physical and transcriptional map of the SPG9 locus on 10q23.3-q24.2.** *Eur J Hum Genet* 2000, **8:**777-782
56. Verhoeven K, Villanova M, Rossi A, Malandrini A, De Jonghe P, Timmerman V, Saitoh T and Katoh M **Localization of the gene for the intermediate form of charcot-marie-tooth to chromosome 10q24.1-q25.1.** *Am J Hum Genet* 2001, **69:**889-894
57. Jeon S and Lambert PF **Integration of human papillomavirus type 16 DNA into the human genome leads to increased stability of E6 and E7 mRNAs: implications for cervical carcinogenesis.** *Proc Natl Acad Sci U S A* 1995, **92:**1654-1658
58. Luft F, Klaes R, Nees M, Durst M, Heilmann V, Melsheimer P and von Knebel Doeberitz M **Detection of integrated papillomavirus sequences by ligation-mediated PCR (DIPS-PCR) and molecular characterization in cervical cancer cells.** *Int J Cancer* 2001, **92:**9-17
59. Einstein MH, Cruz Y, El-Awady MK, Popescu NC, DiPaolo JA, van Ranst M, Kadish AS, Romney S, Runowicz CD and Burk RD **Utilization of the human genome sequence localizes human papillomavirus type 16 DNA integrated into the TNFAIP2 gene in a fatal cervical cancer from a 39-year-old woman.** *Clin Cancer Res* 2002, **8:**549-554
60. Wentzensen N, Ridder R, Klaes R, Vinokurova S, Schaefer U and Doeberitz MK **Characterization of viral-cellular fusion transcripts in a large series of HPV16 and 18 positive anogenital lesions.** *Oncogene* 2002, **21:**419-426
61. Durst M, Croce CM, Gissmann L, Schwarz E and Huebner K **Papillomavirus sequences integrate near cellular oncogenes in some cervical carcinomas.** *Proc Natl Acad Sci U S A* 1987, **84:**1070-1074
62. Reuter S, Bartelmann M, Vogt M, Geisen C, Napierski I, Kahn T, Delius H, Lichter P, Weitz S and Korn B **APM-1, a novel human gene, identified by aberrant co-transcription with papillomavirus oncogenes in a cervical carcinoma cell line, encodes a BTB/POZ-zinc finger protein with growth inhibitory activity.** *Embo J* 1998, **17:**215-222
63. Koopman LA, Szuhai K, van Eendenburg JD, Bezrookove V, Kenter GG, Schuuring E, Tanke H and Fleuren GJ **Recurrent integration of human papillomaviruses 16, 45, and 67 near translocation breakpoints in new cervical cancer cell lines.** *Cancer Res* 1999, **59:**5615-5624
64. Sastre-Garau X, Favre M, Couturier J and Orth G **Distinct patterns of alteration of myc genes associated with integration of human papillomavirus type 16 or type 45 DNA in two genital tumours.** *J Gen Virol* 2000, **81:**1983-1993
65. Thorland EC, Myers SL, Persing DH, Sarkar G, McGovern RM, Gostout BS and Smith DI **Human papillomavirus type 16 integrations in cervical tumors frequently occur in common fragile sites.** *Cancer Res* 2000, **60:**5916-5921
66. Korenberg JR, Chen XN, Sun Z, Shi ZY, Ma S, Vataru E, Yimlamai D, Weissenbach JS, Shizuya H and Simon MI **Human genome anatomy: BACs integrating the genetic and cytogenetic maps for bridging genome and biomedicine.** *Genome Res* 1999, **9:**994-1001
67. Eccles MR, Wallis LJ, Fidler AE, Spurr NK, Goodfellow PJ and Reeve AE **Expression of the PAX2 gene in human fetal kidney and Wilms' tumor.** *Cell Growth Differ* 1992, **3:**279-289
68. Fracchiolla NS, Lombardi L, Salina M, Migliazza A, Baldini L, Berti E, Cro L, Polli E, Maiolo AT and Neri A **Structural alterations of the NF-kappa B transcription factor lyt-10 in lymphoid malignancies.** *Oncogene* 1993, **8:**2839-2845
69. ten Hoeve J, Morris C, Poustka A, Groffen J and Heisterkamp N **Isolation of NotI sites from chromosome 22q11.** *Genomics* 1993, **18:**588-597
70. Morris C, Luppi M, McDonald M, Barozzi P and Torelli G **Fine mapping of an apparently targeted latent human herpesvirus type 6 integration site in chromosome band 17p13.3.** *J Med Virol* 1999, **58:**69-75
71. Crossen PE, Morrison MJ, Rodley P, Cochrane J and Morris CM **Identification of amplified genes in a patient with acute myeloid leukemia and double minute chromosomes.** *Cancer Genet Cytogenet* 1999, **113:**126-133